# INFLUENCE OF STRUCTURE UNIFORMITY OF NANOFIBROUS FILTERS ON THEIR HOMOGENEITY OF FILTRATION EFFICIENCY

Petr BILEK, Jakub HRŮZA

*Technical University of Liberec, Liberec, Czech Republic, EU, petr.bilek@tul.cz, jakub.hruza@tul.cz*

**Abstract**

This paper deals with an influence of structure features of nanofibrous filters on their filtration efficiency. Nanofibrous filtration textiles are made by electro-spinning and different conditions cause different filter structures and pore size distributions. These materials are non-woven and they are composed of individual fibers which lay in an unorganized way. This structure is not uniform as a sieve, but it includes places with higher and lower fiber density which decreases filtration efficiency. The uniformity of a filter is commonly measured under an electron microscope. In this article, the uniformity is determined on the basis of measurement of the filtration efficiency versus position. Woven and nanofibrous nonwoven filtration materials are tested by submicron artificial particles and compared to each other. Experiments were realized on the water filtration setup which allows an optical entrance to the place where a sample of filter is situated.

**Keywords:** Nanofibrous filter, filtration setup, water filtration, flow visualization

## 1. INTRODUCTION

Filtration is a process of separating dispersed phase from another phase. It is separation of solid or fluid contaminants from gas or solid contaminants from fluid. In the filtration process, particle or droplet size has the critical influence on separating. The particles of a certain size pass through the filter, while the larger particles are captured either on the surface or inside of the filter. A filtration material should be strong, flexible, resistant to corrosion and abrasion, easily manipulated and available in a range of porosities.

The filtration process can be divided into several categories according to certain parameters. According to filtration mechanism: surface and depth filtration, according to size of separated particles: hyper-filtration, nano-filtration, ultra-filtration, micro-filtration and particle-filtration, according to used structure of a filter: granular filters, textile filters and membranes. The filtration textile can be divided into woven or nonwoven. In this article, the ultra/micro-filtration of a fluid by the surface nonwoven nanofibrous filtration textiles is discussed. Fluid treatment is indispensable segment of commercial or industrial applications and can be divided into oil filtration (hydraulic oils, fuel) and water filtration. The water filtration involves filtration of ground water into drinking water, washing of waste water, purification in food and beverage production or pharmaceutical processes. Sieve mechanism and consequently size distribution of pores and mean and maximal pores are the key factors in water filtration process. More about the filtration can be found in the literature [1].

Structure of the non-woven filtration textiles is not totally uniform as a sieve for example. It includes places with higher and lower fiber density. The different fiber density is caused by charge pattern of surface where the fibers lie. The uniformity could be determined on the basis of a measurement of the filtration efficiency versus position. For the measuring of filtration parameters, several tests were performed on a water-filtration setup. The setup allows to measure filtration efficiency versus time and position on the basis of visualization of the filtration process. Therefore the measurement enables to determine filtration efficiency of a sample in every place in his surface.

## 2. NANOFIBROUS MATERIALS

Nanofibrous filtration materials are mainly composed of nanofibers. A nanofiber is defined as a sufficiently long fiber with diameter below 1 μm. The nanofibrous textile is made from randomly deposited nanofibers.

There are more ways to produce polymeric nanofibers. Drawing method is based on pulling nanofiber from a polymeric drop by a micropipette and deposited on the surface. Nanofibers are made with help of micromanipulator one after another. Template synthesis method consists of using a template and nanofibers rise by extrusion of the polymer through a porous membrane. Melt-blown technology is based on this principle. In phase separation method, a polymer is mixed with a solvent and after gelation of the polymer is the solvent removed. Pore structure is the result. Self-assembly method is based on intermolecular forces which create nanofibers itself. The last method of nanofibrous production is electrospinning which is briefly discussed below and in more detail described in [2 and 3].

### 2.1 Electrospinning

Advantages of the electrospinning lie in versatile manner of production, also in very narrow (units of nm) and very long (tens of centimeters) fibers. Other advantages are in choice of control features of produced fibers as their diameter, orientation and shape. The principle rests in drawing of a fiber from a drop on a pipette by electrostatic forces. The micropipette serves as the positive electrode and a grounded target is the negative electrode. Industrial production is based on Nanospider method where the nanofibers are electrospinned from free polymer surface.

### 2.2 Investigation of a structure of a nanofibrous filtration medium

Basic properties of nanofibrous textiles are: morphology, molecular structure and mechanical features. Morphological properties of water filter include: pore geometry, size, density and distribution, features of fibers, porosity, wettability, pressure drop and thickness. Nanofibrous textiles have interesting properties as low basis weight, high porosity and smaller pore size comparing to microfibrous materials.

The first important property is fiber diameter. The diameter is mostly in range of 50 – 2000 nm and can be examined with a scanning electron microscope (SEM). Transmission electron microscope (TEM) without gold coating can be used in case of very thin fibers. Pore size distribution (PSD) and porosity play important role in performance of porous materials. PSD can be determined by a direct method under SEM or by an indirect method as mercury porosimeter. The advantage of the indirect measurement is determination of PSD of a whole membrane not only surface of the sample. Bubble pressure and gas transport method can be also used for measurement of PSD. Its advantages are simpler method of measurement and safer usage without mercury [2 and 4].

Mechanical properties of electrospun polymer nanofibrous media are very important in case of long term durability or cleaning. A single nanofiber can be mechanically tested, but this method has its limitations. It is better to test tensile properties of whole nanofibrous membrane. A tensile apparatus is used for testing tensile properties in various speeds. Results are significantly influenced by fiber orientation, diameter and polymer type.

### 2.3 Water filtration by a nanofibrous filter

Nanofibers in the form of membrane have wide range of utilization. Filtration of air by nanofibrous materials was described in several articles, for example in [5, 6]. In this article, only the filtration purpose (especially the water filtration) is discussed. Water filtration is more difficult due to its higher viscosity $\eta_{water} = 1.12 \cdot 10^{-3}$ Pa·s (15 ˚C) compared to air $\eta_{air} = 1.81 \cdot 10^{-5}$ Pa·s (15 ˚C). Water filtration process is more energy consuming, slower. Membranes for water filtration have lower flux and higher fouling. However, nanofibers materials are suitable candidates for filtration applications as pre-filters, more in [8].

In the article [7], a polyvinylidene flouride electrospun membrane was tested in water filtration. This material is commonly used in developing microfiltration membranes. Polystyrene (PS) microspheres of 1, 5 and 10 um in size were used for testing the filter. Presence of any particles in downstream of the filter for each 5 ml of permeate was detected by UV spectrophotometry and the concentration was calculated via calibration curve. Results were filtration efficiency, pressure drop and flux versus time for each size of artificial particles. Nanofibrous filter is capable to remove mono-disperse seeding particles in range of 5 – 10 um effectively without any damage.

In the paper [8], a polyethersulfone (PES) electrospun nanofiber medium was also tested in liquid separation due to its high thermal, chemical and mechanical resistance and technical non-woven PET was used as a sub-layer. PES electrospun nanofibers were at first analyzed under SEM. PSD was measured by an automated capillary flow porozimeter. Permeability and structural stability were examined by water flux measurements. Result was permeation $J$ [liter/m$^2$·hour]. Then the retention tests with poly-disperse PS particle suspensions with sizes below 1 um and above 1 um were performed. Particle size distributions and concentrations were measured by a particle size analyzer. The result was that the bigger particles from suspension above 1 um were rejected without blocking the pores. This behavior is very promising in pre-filtering. On the other hand, suspension below 1 um caused significant decrease of flux and made dense cake layer

## 3. PRINCIPLE OF THE MEASUREMENT

Filtration efficiency is commonly measured by detecting concentration of particles of upstream $C_1$ and downstream $C_2$. Concentration of particles is measured by optical particle counters. These common methods cannot describe morphology of a tested filter. Morphology is quantified only on the basis of optical or electron microscopy. In this article, morphology of the filter is described on the basis of measurement of spatial filtration efficiency. Spatial filtration efficiency is also valuable information about filter homogeneity.

The first experiments with visualization of flow and filtration efficiency measurement on the basis of image processing were done in [9]. Hardware arrangement of the presented measuring method is very similar to Particle Image Velocimetry (PIV) or Planar Laser Induced Fluorescence (PLIF) measuring methods [10, 11]. An examined medium is seeded up by artificial particles. In a laser sheet, the particles are illuminated and the illuminated particles are captured by a camera. PIV uses double pulse lasers to obtain two images of the flow. In our case, we use continuous laser to obtain only single images of a flow through a filter. PLIF method uses fluorescent particles to catch fluorescent light. In this article, the polystyrene non-fluorescent seeding particles are used for measuring filtration properties and at the same time for the visualization of a filtration process.

The more particles are in the medium, the more light is scattered and the area of the picture is brighter. Higher concentration of particles in the medium $C$ [1/liter] ( $C_m$ [g/liter] ) causes higher scattered light intensity $I$ [cd/m$^2$] and it causes higher digital grey value in the image $Y$. Filtration efficiency $EF$ [%] in $x$, $y$ coordinates is consequently calculated:

$$EF(x,y) = 100 \cdot \left(1 - \frac{C(x,y)_2}{C(x,y)_1}\right), \quad (1)$$

where $C_1$ is the concentration of upstream and $C_2$ of downstream of the filter. Calibration curve $C(Y)$ is experimentally obtained for actual settings of the filtration setup and used testing particles. Then local concentration of particles $C(x, y)$ can be determined from the local digital grey value $Y(x, y)$.

## 4. EXPERIMENTAL SETUP

Experimental setup was constructed according to scheme in Fig. 1. Filtration apparatus is composed from 3 circuits. The first circuit is a bypass and serves only for raw control of flow in circuit 2. The sample of a

filtration material is mounted in measuring circuit 2. Circuit 3 is activated only in case of cleaning of whole filtration apparatus. Range of flow is 0.1 – 20 liters per minute. Pressure drop can be in range 0 – 350 kPa. Diameter of a filtration sample is 5 cm and it is submerged in a glass water tank to prevent light refraction. The filtration process is captured by a digital camera Pike F-210B/C with CCD chip of resolution 1920 x 1080 pixels. Here the laser sheet and the camera are mounted to the one axis traverse mechanism. This arrangement allows investigating whole surface of a filtration sample.

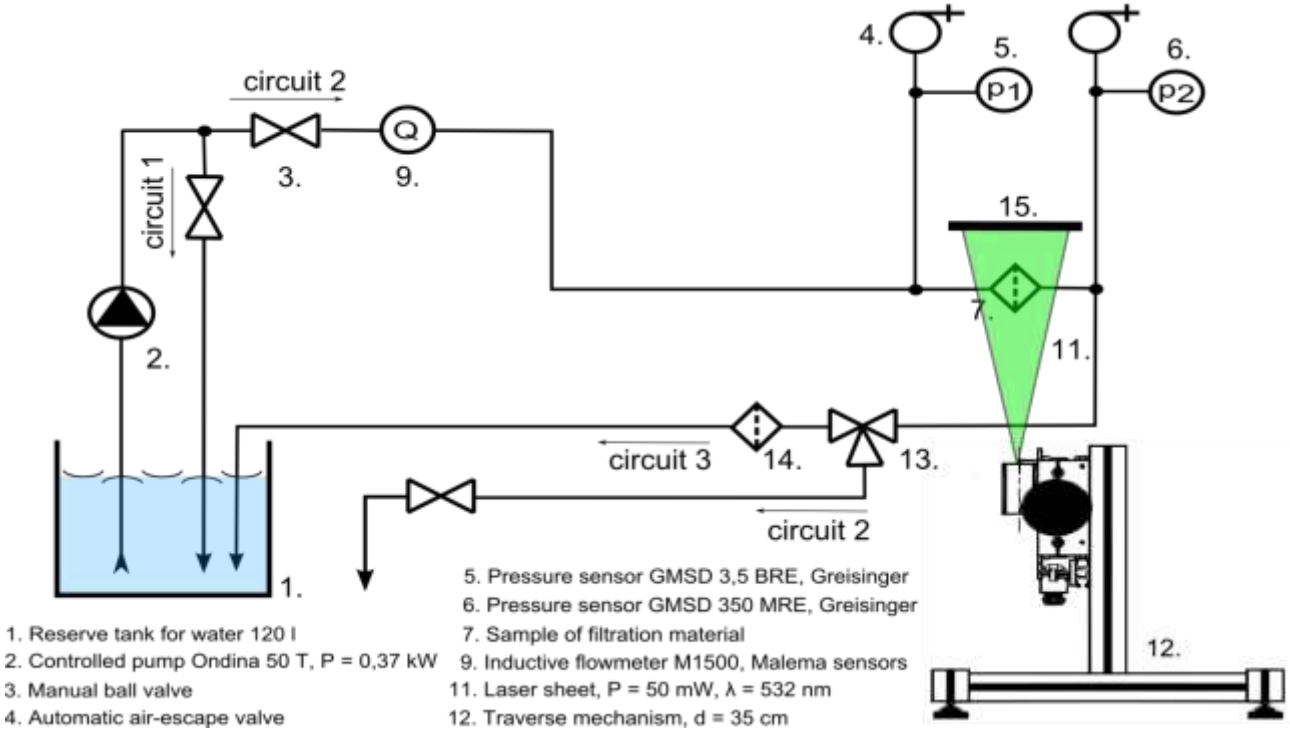


**Fig. 1** Scheme of the filtration setup

**Fig. 2** Picture of the filtration apparatus in laboratory

## 5. PERFORMED TESTS

### 5.1 Parameters of the used materials

Four types of different filtration textiles (needle felt, non-woven meltblown, non-woven nanofibrous and woven) are described in Tab. 1 in detail. Maximum pore and mean pore size were obtained by the bubble point test. Air flow and pressure drop of dry and oiled sample of the textiles were measured. Maximum pore size was obtained from the highest pressure drop when no air flow had been observed. Mean pore size was calculated from the pressure drop where the half air flow curve and the pressure drop curve crossed respectively.

**Table 1** Parameters of the used filtration materials

| filtration textile | needle felt | meltblown | woven | nanofibrous |
|---|---|---|---|---|
| used material | polyester | polypropylen | polyester | polyamid |
| surface weight [g/m$^2$] | - | 35 | - | 0.45 |
| mean pore size [µm] | 42 | 22 | 54 | 9 |
| max pore size [µm] | 109 | 49 | 83 | 56 |
| permeability versus position K | | | | |
| mean value [m·Pa$^{-1}$·sec$^{-1}$] | 0.001214 | 0.0021 | 0.0015 | 0.0007 |
| variation coeficient [%] | 3.1 | 8.3 | 2 | 52.5 |
| confidence 95% [m·Pa$^{-1}$·sec$^{-1}$] | 0.000013 | 0.000058 | 0.00001 | 0.000126 |

The permeability was measured by METEFEM type F-12/A. For each textile of approximate area 0.5 m$^2$, almost 50 values of pressure drop $\Delta p$ and air flow $Q$ were obtained and the permeability

$$K = \frac{Q}{A \cdot \Delta p} \tag{2}$$

was calculated. The round active area was $A$ = 10 cm$^2$. Tolerances of the air flowmeters are ±1.5 %.

Polystyrene microspheres about density 1.05 g/ml and size 0.96 µm were used as seeding particles in this article. They are uniform and spherical and dispose perfect optical parameters as well. They were purchased from company Bang Laboratories, Inc.

### 5.2 Calibration of the setup

Calibration of the setup is very important process and has significant effect on accuracy and repeatability of the consequent measurements. The goal is to find out a curve of $C(Y)$ which is used for expression of concentration of particles $C$ from digital gray value $Y$ from an image of flow. Each pixel of the image or a larger defined area in the image is defined by unique calibration curve. A lot of influences take effect on homogeneity of the image. A laser sheet is not uniform, but contains strips of higher intensity of light, Fig. 3. That is caused by an error of cylindrical lens. A camera error is called vignette and it makes brighter center and darker margin of an image. It is caused by lens mounted on a camera. Optical filtration channel is also not uniform and contains inhomogeneities. All these errors are effectively subdued just by the calibration.

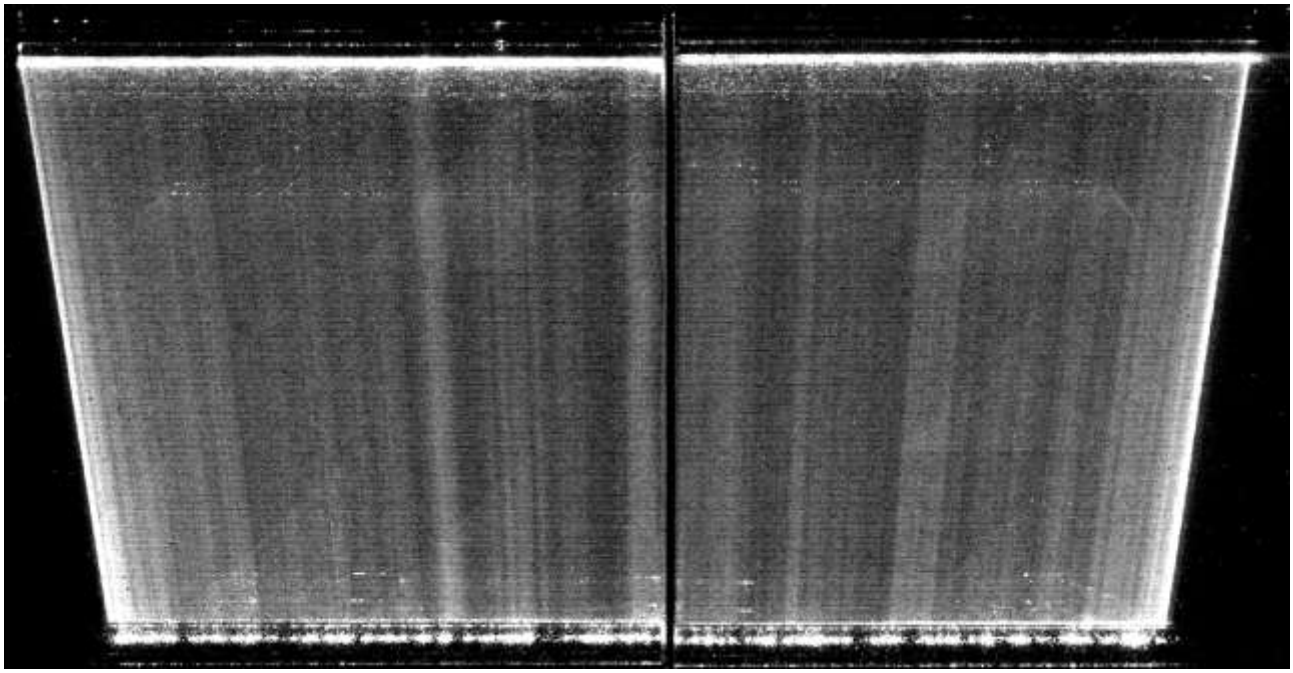

**Fig. 3** Laser sheet with local higher and lower intensity

Calibration was performed in small glass tank (20 x 10 x 15 cm) made from the same glass as the filtration channel. The glass tank is filled by distilled water and concentration of artificial particles is step by step increased from zero to maximum concentration. A couple of images of liquid are obtained for each concentration. Curves $Y(C)$ are expressed from the known concentration and digital grey values of all pixels and the inverse function is searched calibration curve

$$C(x,y) = K(x,y)_T \cdot Y(x,y) + C(x,y)_B, \tag{3}$$

where $K_T$ is calibration constant and $C_B$ is offset. Image analysis was performed in ImageJ software and post-processing in Matlab. Images of impurities (mostly dust and much bigger sized artificial particles) were removed from the pictures in ImageJ software as well.

Light multiscattering and attenuation by seeding particles plays significant role in case of higher concentrations on the linearity of the calibration curve. Calibration curve is linear from zero up to maximum concentration of particles $C_{max}$ = 254 μg/liter as we can see in Fig. 4. After the maximum concentration is reached, the light response becomes non-linear versus concentration of particles, Fig. 5.

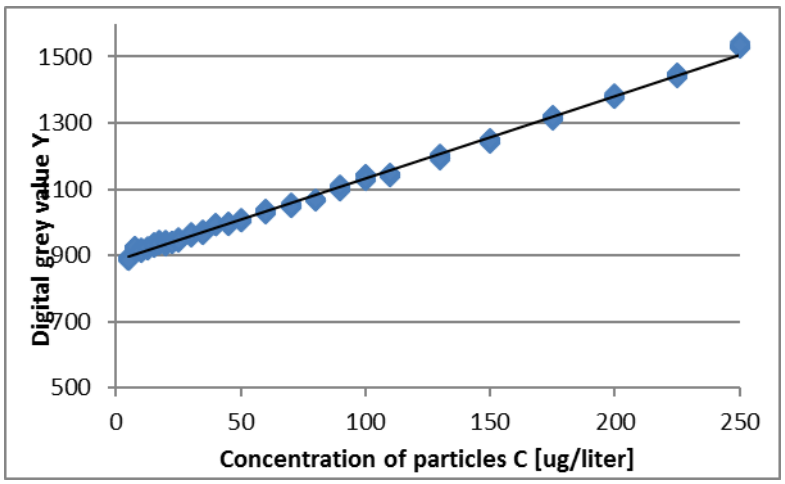

**Fig. 4** Curve of digital grey value versus concentration of particles

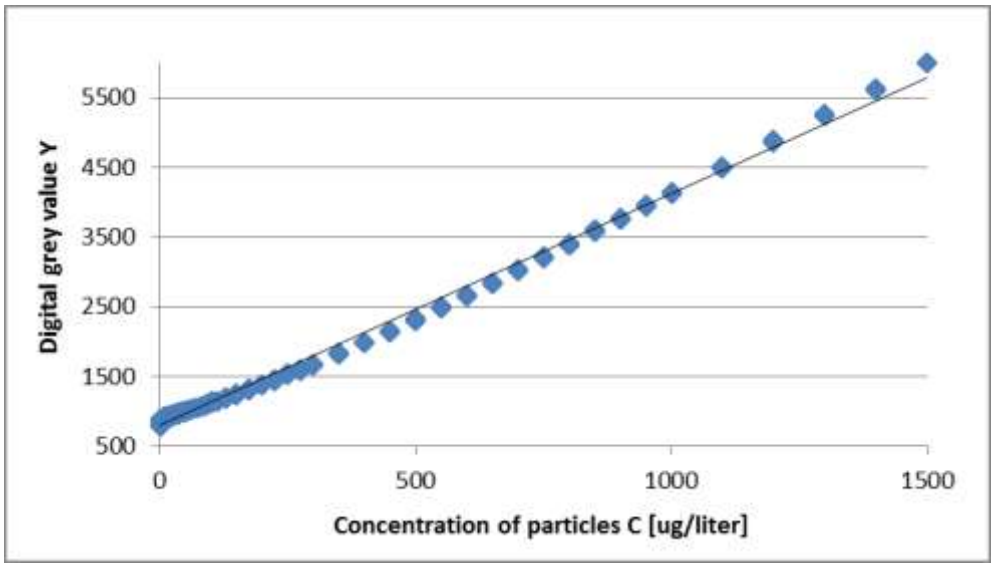


**Fig. 5** Curve of digital grey value versus concentration of particles

### 5.3 Measurement of filtration efficiency versus time and position

At the start of the measurement, 120 liters of distilled water was poured into the reserve tank and circuit 3 is activated. The filtration setup is cleaned by the filter (see Fig. 1 - 14) during 1-2 hours without any sample of tested filter (Fig. 1 - 7). Cleaning is important for ensuring the same conditions of high water purity at the start of the tests. Approximately 100 liters of cleaned water is seeded up by artificial particles of concentration of $C_1$ = 254 µg/liter. Square samples (active area 5 x 5 cm) of all testing filtration textiles were prepared and step by step mounted into the setup between two optical glass filtration channels and tested. Flow was constantly hold on 1 liter per minute and pressure drop was measured by pressure sensors.

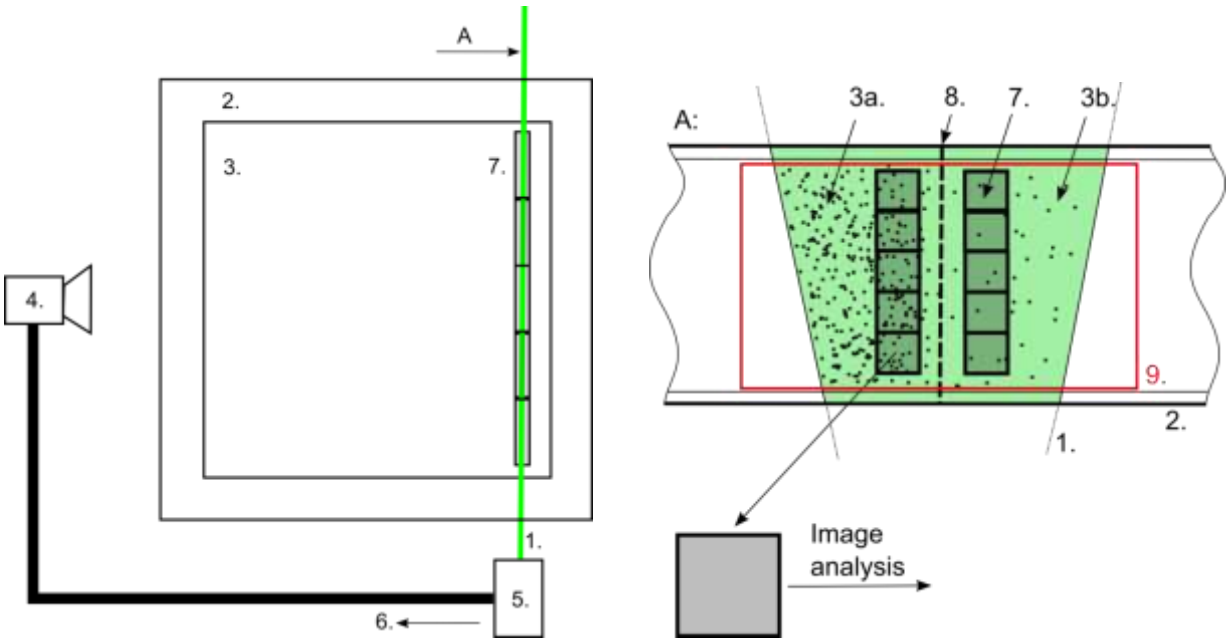


**Fig. 6** Block scheme of the measurement principle: 1: laser sheet, 2: filtration channel from glass, 3: water seeded by artificial particles, 3a: upstream, 3b: downstream, 4: camera, 5: laser unit, 6: direction of the traversing, 7: evaluative areas, 8: sample of a filtration textile, 9: an area of flow seen by the camera

The camera is mounted perpendicularly to the laser sheet. During the tests, images of flow in the vicinity of the filter are recorded to a PC. Images with resolution 1920 x 1080 pixels are composed from 16 bit levels of grey scale pixels. Data format is RAW with the suffix BMP. Gain of the camera was set to maximum 630 and shutter time was set to 20 ms. Aperture of lens was set to F1.4.

The laser sheet and the camera are mounted to a duralumin arm which is fixed with the head of one axis traverse mechanism. During the tests, the arm is traversing from the back to the front and vice-versa, Fig. 6. The traverse mechanism and the camera are controlled by MACA software made by author in NI LabView. Images are loaded from the camera with help of AVT Smart View software by Allied Vision Technologies GmbH.

Image analysis was performed in ImageJ software. An image area close to a sample of the filtration textile is divided into two columns of small evaluative areas each consisting of 100 pixels (1 evaluative area is 10 x 10 pixels), Fig. 6. Concentration of particles is calculated (1) for this each evaluative area through calibration parameters (2).

### 5.4 Comparison of the results and discussion

Results from the measurements are presented as curves in graphs of filtration efficiency versus position, Fig. 7 - 9. The needle felt filter unfortunately did not seal during the experiment due to higher thickness, therefore the results were distorted and they are not presented in the article any more. We can notice that the filtration efficiency of non-woven filtration textiles (meltblown and nanofibrous) is much more inhomogeneous than the filtration efficiency of the woven sample. It is caused by inhomogeneous filtration layer which contains places of more and less fibers. This is also seen on permeability in Tab. 1, where the non-woven filtration textiles (especially nanofibrous filtration textile) have much worse homogeneity of permeability than woven textiles.

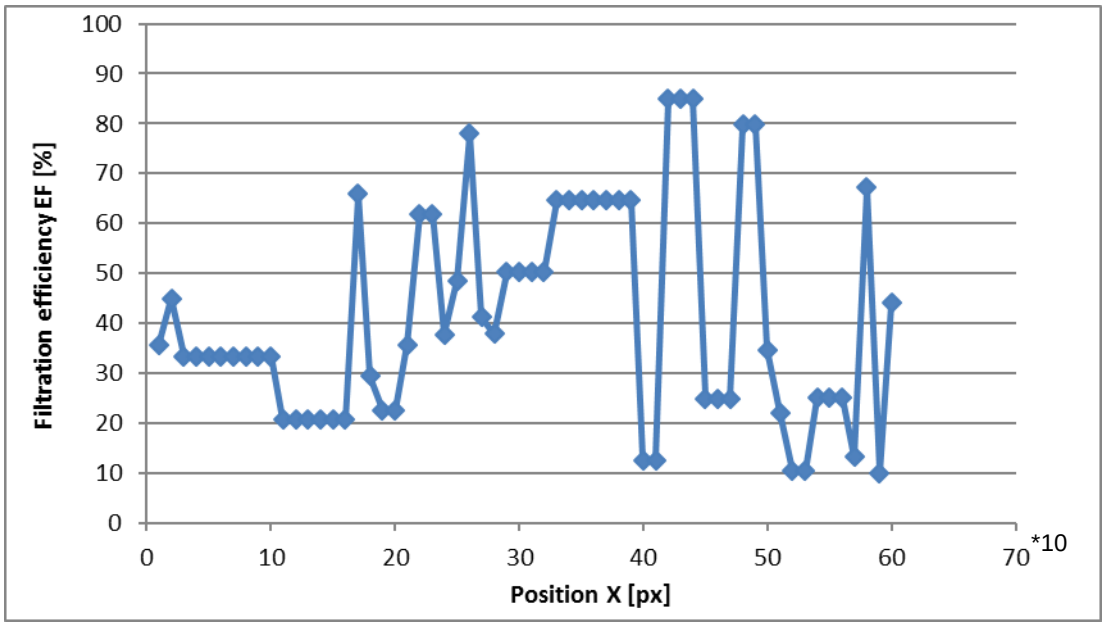


**Fig. 7** Filtration efficiency versus position of non-woven filtration textile (meltblown)

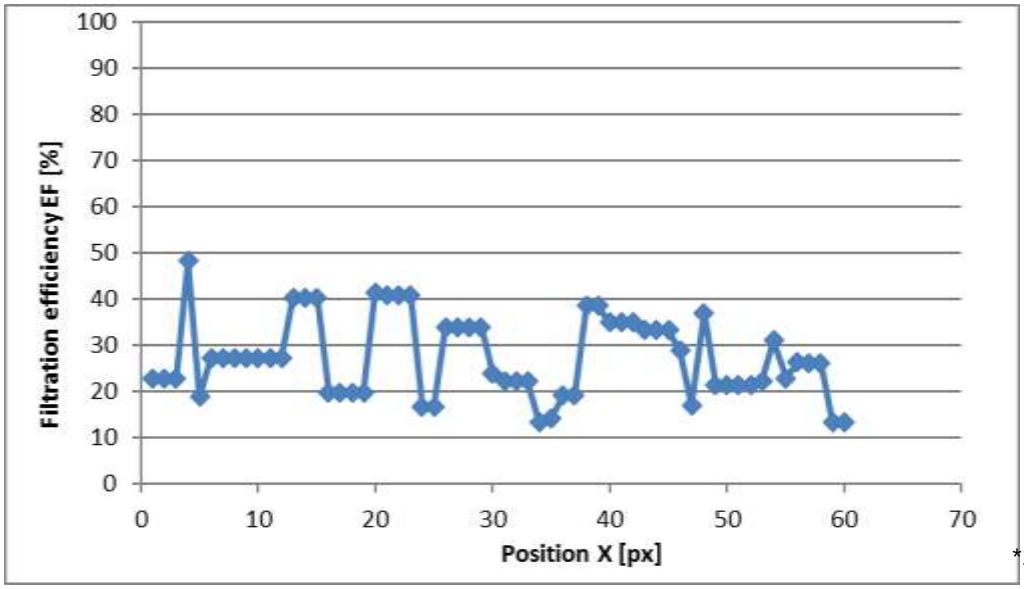


*10

**Fig. 8.** Filtration efficiency versus position of woven filtration textile.

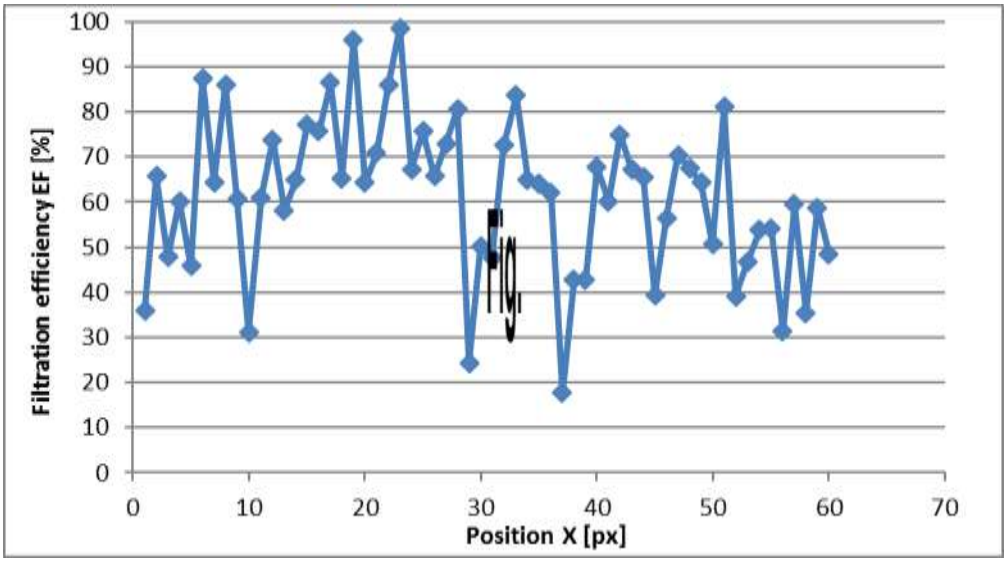


*10

**Fig. 9.** Filtration efficiency versus position of nanofibrous filtration textile.

The Tab. 2 summarizes the measured results of the homogeneity of filtration efficiency. The woven filtration textile has lower mean filtration efficiency then the non-woven textiles. The higher values of the maximum and mean pore size in Tab. 1 also indicate lower filtration efficiency. Interesting issue is the higher permeability of the non-woven filtration textile. This is probably caused by smaller fibers of the non-woven filter. The nanofibrous filter disposes with the highest mean filtration efficiency because of very small mean pore size.

**Table 2.** Comparison of non-woven (meltblown and nanofibrous) and woven filtration textiles

| filtration efficiency versus position EF | meltblown | woven | nanofibrous |
|---|---|---|---|
| mean value [%] | 41.2 | 27.5 | 61.5 |
| variation coeficient [%] | 52.6 | 31.2 | 28.0 |
| confidence 95% [%] | 5.5 | 2.2 | 4.4 |

## 6. CONCLUSION

PIV and PLIF methods are very strong tools for visualization and quantification of flow. They exist in many variations, however in very special cases, they are not sufficiently suitable. Filtration materials are usually tested by artificial particles with diameter 0.1-10 μm. In this article, flow is seeded by polystyrene spherical particles with diameter 0.96 μm. Applied seeding particles are not fluorescent and they are bigger than typical particles used for PLIF method. Due to this circumstances, a new setup with optical access to the place were a filter is mounted was built. New setup allows to measure filtration efficiency in time versus position and then to determine filtration parameters.

The measured results of the filtration efficiency by new filtration setup (Tab. 2) were verified by the measurement of pore size and permeability in position, Tab 1. Non-woven filtration textiles (meltblown and nanofibrous) have smaller pore size (Tab. 1) and higher mean filtration efficiency (Tab. 2). The non-woven filtration textiles have higher variance in permeability (Tab. 1). Also higher variance in filtration efficiency (Tab. 2) was measured by the new filtration setup. These results agree with each other. In the graphs in Fig. 7 - 9, curves of filtration efficiency versus position are compared to each other. Woven textile disposes smoother curve than non-woven filters (meltblown and nanofibrous). This is caused by the production technology. Non-woven structure is uniform as a sieve compared to a non-woven textile where the fibers are laid in an unorganized way. The performed measurements approved that the direct observation method of the filtration process is able to indicate inhomogeneities of the filtration layer.

## ACKNOWLEDGEMENTS

***This work was supported by the Ministry of Education of the Czech Republic within the SGS project no. 21066/115 on the Technical University of Liberec.***

## REFERENCES

[1] SUTHERLAND, K. Filters and Filtration Handbook. Elsevier. Oxford. 2008. p. 523. ISBN 978-1-8561-7464-0.

[2] RAMAKRISHNA S., FUJIHARA K., TEO W. E., LIM T. C., MA Z. An Introduction to electrospining and nanofibers. World Scientific Publishing Co. Pvt. Ltd. 2005. p. 382. ISBN 981-256-415-2.

[3] JIRSÁK O., SANETRNÍK F., LUKÁŠ D., KOTEK V., MARTINOVÁ L., CHALOUPEK J. A method of nanofibres produsction from a polymer solution using electrostatic spinning and a device for carrying out the method. European patent specification. Liberec. 2004.

[4] NAKAO, S. Determinaion of pore size and pore size distribution 3. Filtration membranes. Journal of Membrane Science 96. 1994. 131 – 165.

[5] BARHATE, R.S., RAMAKRISHNA, S. Nanofibrous filtering media: Filtration problems and solutions from tiny materials. Journal of Membrane Science 296. 2007. p. 1 – 8.

[6] PODGÓRSKI, A., BALAZY, A., GRADÓN, L. Application of nanofibers to improve the filtration efficiency of the most penetrating aerosol particles in fibrous filters. Chemical Engineering Science 61. 2006. p. 6804 – 6815.

[7] GOPAL, R., KAUR, S., MA, Z., CHAN, C., RAMAKRISHNA, S., MATSUURA, T. Electrospun nanofibrous filtration membrane. Journal of Membrane Science 281. 2006. p. 581 – 586.

[8] HOMAEIGOHAR, S.Sh., BUHR., K., EBERT, K. Polyethersulfone electrospun nanofibrous composite membrane for liquid filtration. Journal of Membrane Science 365. 2010. p. 68 – 77.

[9] JAŠÍKOVÁ, D., KOTEK, M., ŠIDLOF, P., HRŮZA, J., KOPECKÝ, V. Vyhodnocování nanofiltru vizualizačními metodami. konference Nanocon, 2009. p. 186-190. ISBN 978-80-87294-13-0.

[10] TORRES, L. A., FLECK, B. A., WILSON, D. J., NOBES, D. S. Calibration of a planar laser induced fluorescence technique for use in large scale water facilities. Measurement 45. 2013. p. 2597 – 2607.

[11] KOPECKÝ, V. Laserové anemometrie. Technická Univerzita v Liberci, 2006. p. 186. ISBN 9788070839454.